Perforation Tests of Aluminum Alloy Specimens for a Wide Range of Temperatures Using High-Performance Thermal Chamber - Experimental and Numerical Analysis

IOP Conf. Series: Materials Science and Engineering **491** (2019) 012027 doi:10.1088/1757-899X/491/1/012027

Perforation Tests of Aluminum Alloy Specimens for a Wide Range of Temperatures Using High-Performance Thermal Chamber - Experimental and Numerical Analysis

A. Bendarma [1, 2, *], T. Jankowiak [1], A. Rusinek [3] and T. Lodygowski [1] and M. Klosak [, 2]

[1]Poznan University of Technology, Institute of Structural Engineering, Piotrowo 5, 60-965 Poznan, Poland
[2]Universiapolis, Ecole Polytechnique d'Agadir Bab Al Madina, Qr Tilila, Agadir, Morocco
[3]National Engineering School of Metz, Laboratory of Mechanics, Biomechanics, Polymers and Structures, 1 route d'Ars Laquenexy, 57000 Metz, France

[*]E-mail address: b.amine@e-polytechnique.ma, Tel: +212-6-61-09-88-72

Abstract. The paper describes a work focused on the process of perforation of aluminum alloy sheet at a wide range of specimen temperatures. This has been obtained by using the specially designed thermal chamber to heat specimens before impact. Based on this experimental series. Experimental, analytical and numerical investigations have been carried out analyze the perforation process, the ballistic properties of the aluminum alloy impacted by a conical nose shape projectile are studied. The experimental investigations have been extended by numerical simulations using a general purpose software Abaqus/Explicit. A good correlation has been obtained. To study the temperature effects. The range of available temperatures is from the room ambient temperature up to 300 ˚C. The time needed to heat the specimen and to stabilize its temperature is 20 minutes. This study has allowed to discuss the ballistic behavior and resistance of sheet plates of the aluminum alloy under dynamic loading and different temperatures.

1. Introduction

In the international literature has been a few experimental data available in which specimens are subjected to impact loading at elevated temperatures. The usual approach is to carry out perforation tests at room temperature and to extrapolate results using numerical simulations at high temperatures.

Many authors have deal with perforation analysis, from theoretical approaches such as discussed in [1-2] to more practical considerations as reported in [3-5]. [6-8] studied the influence of the projectile nose shape (conical, blunt and hemispherical) and the projectile diameter on ballistic properties and failure modes of thin steel targets. In order to simulate the behavior of impacted and perforated structures, the finite element method with an explicit time integration procedure was an effective technique. [6-10] Numerical simulations, in particular by the FE method, are also effective supplements for theoretical and experimental investigations which were carried out to analyze the dynamic behavior of impacted materials. However, no direct data concerning perforation failure modes at high temperatures are reported or published. The thermal softening of the material is usually

tested using quasi-static experiments and its extrapolation to high strain rates is often a rough simplification. The idea of carrying out dynamic tests using thermal chamber is a solution of the problem. In this work, a new highly-performant thermal chamber is used to heat up metallic thin plate specimens and to impose an initial temperature higher than the room temperature. The maxi-mum temperature reached with this original device is 300 ˚C. Aluminium alloy has been selected in this work due to it no or insignificant strain rate sensitivity [11]. Experimental results obtained have been compared with available literature data.

2. Equipment for specimens heating

To reach a perforation tests at high impact velocity, a pneumatic gas gun has been used (Figs 1 and 2). It permits to reach a maximum initial impact velocity V_0 of 125 m/s for a projectile mass equal to $m_p = 28$ g. During this work, the present device is equipped with a thermal chamber. The temperature may vary from room temperature to 300 ˚C. A waiting time of about t≈20 min was estimated to heat up the specimen and to reach a uniform temperature distribution in the specimen. For it, a thermocouple was fixed in the middle of the reference plate to calibrate the thermal chamber. Another thermocouple was fixed inside the thermal chamber to enable a homogenous temperature control. Using the previous set-up described, Aluminum alloy plates have been subjected to perforation. The plate dimensions were $130\ \text{mm} * 130\ \text{mm}$ for thicknesses equal to t=1 mm. Which is fixed along its perimeter to provide a perfect fixation and to avoid sliding. The gas gun set-up is shown in Figure 1.

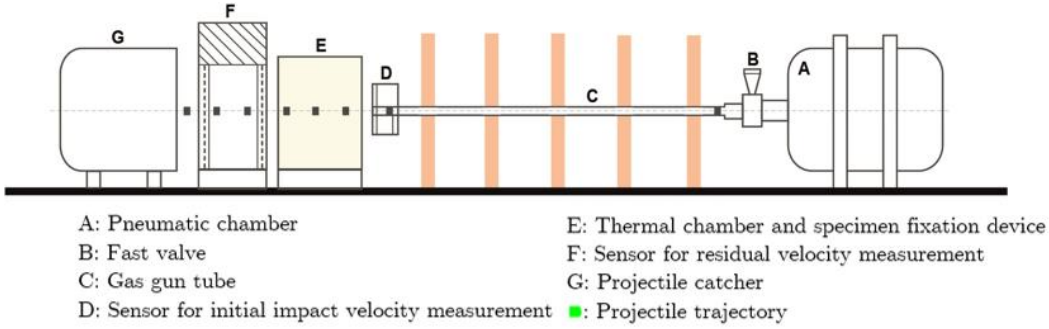

Figure 1. Gas gun set-up used for perforation tests at high impact velocities and temperatures [12]

A wide range of impact velocities from 40 to 125 m/s has been covered during the tests. The oven used for the test is presented Figure 2. A sarcophagus is used around the plate specimen to have a uniform temperature distribution after a certain waiting time. Therefore, the two sides of the specimen are heat up in the same time. After it, due to conductivity the entire specimen is heated to reach the initial temperature imposed.

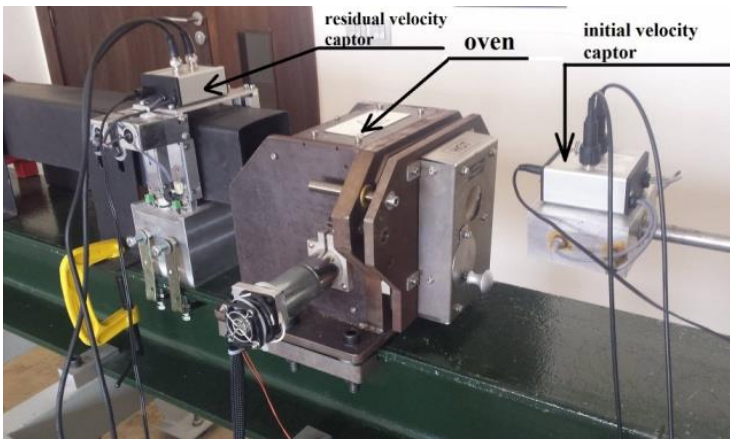

Figure 2. Oven used for perforation tests at high impact velocity and high temperature.

3. Experimental results

3.1. Perforation test at room temperature

In this section the mechanical behavior of aluminum sheets under impact loading has been described. Experimental, analytical and numerical investigations have been carried out to analyze the perforation process [6]. A wide range of impact velocities from 40 to 180m/s and temperature from 21 to 300 ˚C has been covered during the tests. The residual velocity of the projectile can be calculated using the equation proposed by [13] Eq.1,

$$V_R = (V_0{}^{\kappa} - V_B{}^{\kappa})^{1/\kappa}, \tag{1}$$

Where V_0 is the initial velocity, the constant V_B is equal to 40 m/s, and the ballistic curve shape parameter k is equal to 1.65, the absorbed energy by the plate E_d can be calculated using Eq.2

$$E_d = \frac{m_P}{2}\left(V_0{}^2 - V_R{}^2\right). \tag{2}$$

The results in terms of the ballistic curve V_R-V_0 are reported in Fig. 3a.

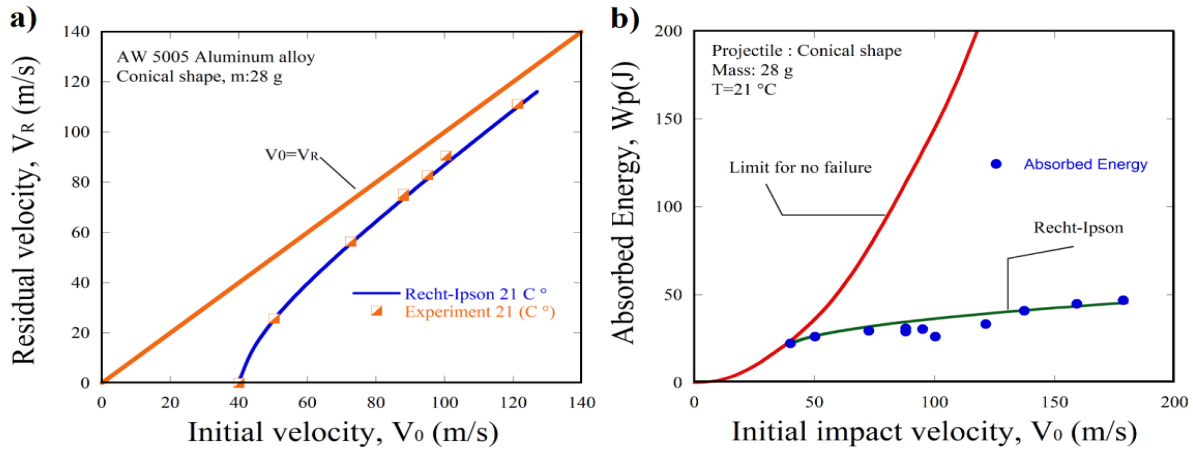

Figure 3. a) Ballistic curve obtained during perforation and determination of the ballistic limit, b) Energy absorbed by the plate during impact test, determination of the failure energy,[12]

The difference of the initial and residual kinetic energy can be calculated using the experimental data, then based on the Recht-Ipson approximation, the energy absorbed by the plate can be calculated, see Fig. 3b. Using Eq.2 the minimum energy to perforate is 28 J ($m_P = 28\ g$ and $V_0 = V_B = 40\ m/s$).

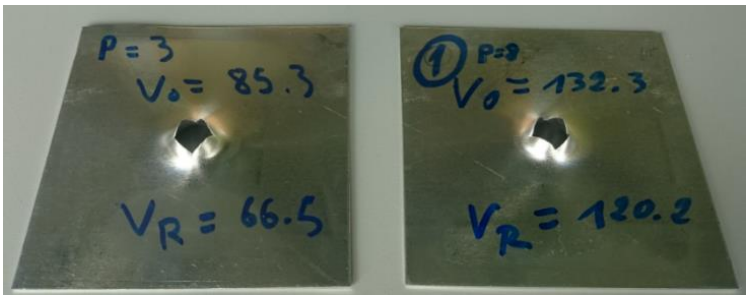

Figure 4. Experimental observation of failure patterns, V_0= 85.3 m/s and 132.3 m/s, [12]

As showed in Figure 4 for the initial impact velocity of V_0 = 85 m/s the failure pattern has been obtained with four petals with the residual velocity of $V_R = 66.5$ m/s. The same failure is observed for the V_0 = 132.3 m/s with $V_R = 120.2$ m/s, respectively, the number of petals is equal to 4 from 40 to 125 m/s. [14] contain a complete description concerning the number of petals depending on the projectile shape and the failure mode.

3.2. Perforation test at elevated temperature:

To complete this work a based ballistic studies have been performed. Experimental results in term of the failure mode are reported. A typical failure behavior are observed, the failure modes observed depends on both impact velocity and initial temperature value. Using a conical projectile, a failure mode by petaling occurs inducing radial necking due to a process of piercing. The conical projectile perforates the target plate and the plastic strain is localized at the extremities of the petals. Analytical predictions discussed in [15] are fully confirmed at room temperature, whereas more discrepancy in petals number is reported at higher temperatures. Figure 5 present a comparison between experimental results at room temperature and for a temperature of 100 and 300 ˚C for 1 mm plate thickness. It can be observed that increasing the initial temperature of the specimen changes the ballistic limit (no perforation state) to lower values: the ballistic limit obtained is approximately 40 m/s (20 ˚C), 35 m/s (100 ˚C), 34 m/s (200 ˚C) and 32 m/s (300 ˚C) using the conical projectile. Whereas the shape parameter k is 2.1 (100 ˚C), 1.83 (200 ˚C), 1.9 (300 ˚C) respectively. The other measured points are also shifted when higher residual velocities V_R are measured for elevated temperatures. The energy absorbed during the impact does not change considerably with the impact velocity. Experimental results stay in accordance with analytical predictions using Eq. 2 [13].

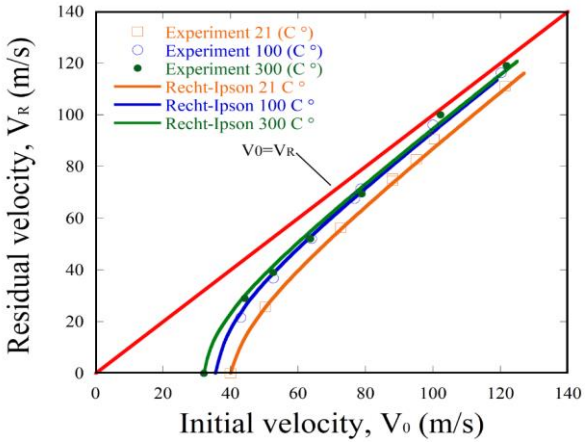

Figure 5. Impact velocity V_0 vs residual velocity V_R - experimental results for T=21˚C, T=100˚C and T=300˚C; using conical projectiles

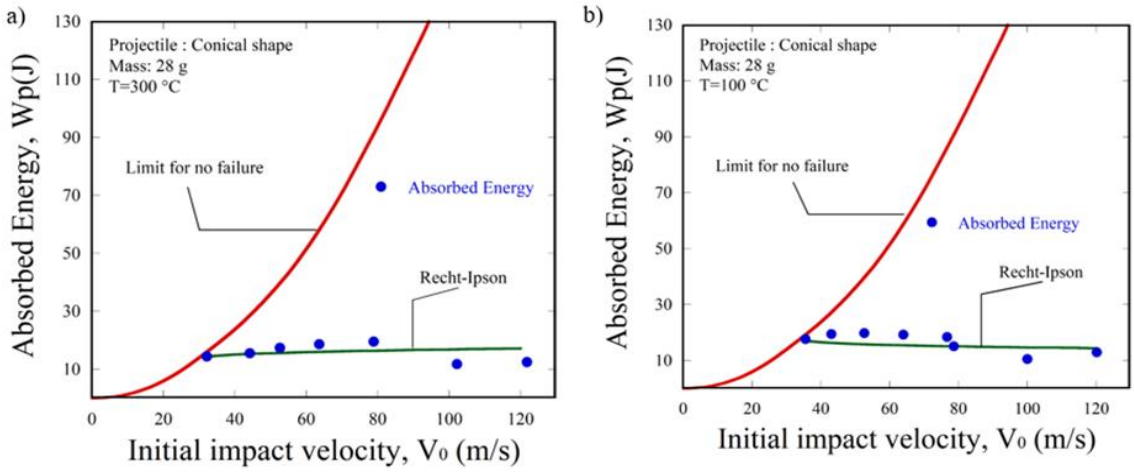

Figure 6. Energy absorbed by the plate during impact test, a/ T=100 ˚C and b/ T=300 ˚C; using conical projectile

Perforation process causes an instant increase of temperature localized in the perforated zone. Plastic deformation energy dissipated during the perforation process is transformed into thermal

energy and provokes a considerable increase of temperature in petals. As shown in figure 6 the energy is quite constant at 100 ˚C and 300 ˚C, in the contrary at room temperature the absorbed energy increase when the initial impact velocity increase.

4. Numerical simulation

4.1. Material parameters

In the context of this work's applications, a model has been chosen, it is an empirical model from Johnson-Cook to describe the behavior of the studied material. Johnson and Cook propose an empirical law [16] based on experimental results and designed for rapid implementation in calculation codes. This model includes the influences of deformation velocity; strain hardening and temperature:

$$\sigma = \left(A + B\varepsilon_{pl}^{n}\right)\left(1 + C\, ln\frac{\dot{\varepsilon}^{p}}{\dot{\varepsilon}_{0}}\right)(1 - T^{*m}) \tag{3}$$

Where A is the yield stress, B and n are the strain hardening coefficients, C is the strain rate sensitivity coefficient, $\dot{\varepsilon}_0$ is strain rate reference value and m is the temperature sensitivity parameter. In this work, isothermal conditions are assumed. Therefore, the last term of the JC model related to the non-dimensional temperature where T^* is the homologous temperature.

The material constants are obtained from experimental tests. The Parameter C has been calculated using presented experimental tests for quasi-static loading. These constants are shown in Table. 1 [12].

Table 1. Material parameters for Johnson-Cook model, [12]

A (MPa)	*B* (MPa)	*n* (-)	*C* (-)
147	60	0.9	0.003

4.2. Failure criterion

During our analysis an analytical and numerical approach for the failure criterion was also considered as recently proposed in [13] for this aluminium alloy. Two functions with four constants H, I, J and K are determined using an optimization method (based on algorithm using MATLAB software).

$$\varepsilon_Y\,(\dot{\varepsilon}) = \begin{cases} He^{(I\, log_{10}(\dot{\varepsilon}))} & \dot{\varepsilon} \le \dot{\varepsilon}_{Transmition} \\ J - (K\, e^{\,log_{10}(\dot{\varepsilon})}) & \dot{\varepsilon} \ge \dot{\varepsilon}_{Transmition} \end{cases} \tag{4}$$

Where $\dot{\varepsilon}_{Transmition} = 1\ 1/s$.

The exemplar solution of this system of equations for another metal (Aluminum) reported in [12] is presented in Figure 7.

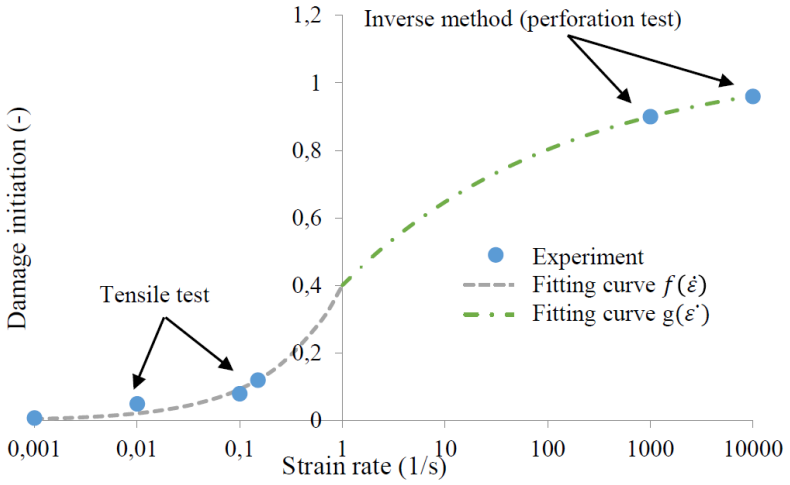

Figure 7. Plot of failure strain versus plastic strain rate using optimized Model III, [12]

4.3. Numerical simulation

Using finite element code Abaqus software the perforation test has been simulated, the mesh is denser in the projectile-plate contact zone, the thickness of the plate in this area is 1.0 mm, and the velocity is defined in the predefined fields with impact velocities range from 40 to 125 m /s as obtained in experiment. The projectile behavior has been defined as rigid body. The friction coefficient is assumed to be equal to 0.2 [12]. When the value of failure strain is changed, a decrease in petals numbers with a 72 ° nose angle has been observed. An analytical model for the number of petals prediction proposed by [14] has been used and confirmed by FE simulations.

5. Results and discussion

In this section a comparison between experimental and numerical results has been done. As it might be seen in Figure 8, there is a good correlation between the experimental and numerical results, the numerical model has demonstrated more ductile behavior at the failure start, it has revealed ductility at the terminal phase of failure.

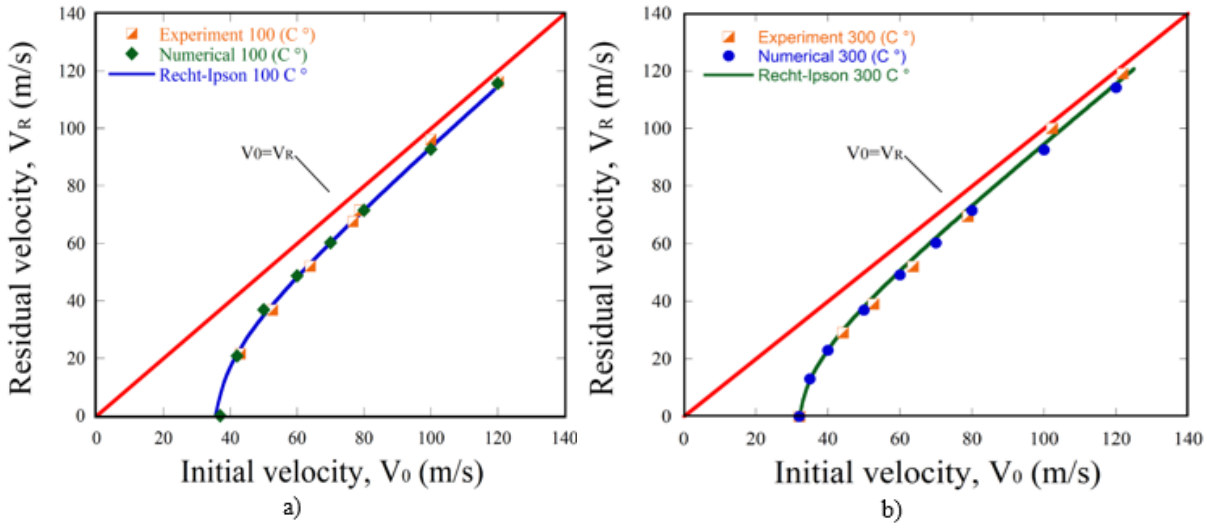

Figure 8. The ballistic curve in experiment and in simulation using thermal condition a/ T=100 ˚C, b/ T=200 ˚C and b/ T=300 ˚C; using conical projectile

It can be concluded that the thermal chamber set-up proved its designed performances and opened new perspectives to carry out perforation tests in a wide range of temperatures. Important results were obtained for aluminum alloy AW 5005 heated to elevated temperatures. The failure mode in form of petals confirmed analytical considerations. The studies on initial impact velocity and residual impact velocities reproduced typical behavior of material. The energy absorbed during perforation is quasi-constant for the studied range of velocities (up to 121 m/s). Using conical shaped projectile, the average value was 26 J at room temperature and decreased to the average of 18 J at 300 ˚C.

6. Concluding remarks

The analysis of the experimental results shows that the material is very strain rate and temperature sensitive. It has been shown in the stress range ($10^{-4}\ s^{-1} \leq \dot{\varepsilon} \leq 10^{4}\ s^{-1}$). The experimental study also showed that temperature has a significant influence on the mechanical behavior. Experiments have shown that the ballistic limit and the failure mode of the structure are strictly related to the projectile's nose shape. A specific analysis shown that the number of petals after perforation increases with the conical angle of the projectile. In the end, a simulation and a numerical analysis to reproduce the experimentally observed dynamic mechanical behavior for the studied structure, has been achieved using the Abaqus finite element code.

References

[1] Børvik, T., Hopperstad, O.S., Langseth, M., Malo, K.A., (2003), Effect of target thickness in blunt projectile penetration of Weldox 460 E steel plates, *International Journal of Impact Engineering*, 28 (4), pp. 413-464.

[2] Recht, R.F., Ipson, T.W. (1963), Ballistic perforation dynamics, *Journal of Applied Mechanics*, 30 (3), pp. 384-390.

[3] Abed, F. H., Voyiadjis, G. (2007), Adiabatic Shear Band Localizations in BCC Metals at High Strain Rates and Various Initial Temperatures, *Int. J. Multiscale Comput. Eng*., 5 (3–4), pp. 325–349.

[4] Jankowiak, T., Rusinek, A., K.M. Kpenyigba, Pesci, R. (2014), Ballistic behavior of steel sheet subjected to impact and perforation. Steel and Composite Structures, 16 (6), pp. 595-609.

[5] Jankowiak, T, Rusinek, A, Wood.P, (2015), A numerical analysis of the dynamic behaviour of sheet steel perforated by a conical projectile under ballistic conditions. *Finite Elements in Analysis and Design*, 65, pp. 39-49.

[6] Kpenyigba, K. M., Jankowiak, T., Rusinek, A., & Pesci, R. (2013). Influence of projectile shape on dynamic behavior of steel sheet subjected to impact and perforation. *Thin-Walled Structures*, *65*, 93-104.

[7] Rusinek, A., Rodríguez-Martínez, J. A., Arias, A., Klepaczko, J. R., & López-Puente, J. (2008). Influence of conical projectile diameter on perpendicular impact of thin steel plate. Engineering Fracture Mechanics, 75(10), 2946-2967.

[8] Rusinek, A., Rodriguez-Martinez, J. A., Klepaczko, J. R., & Pęcherski, R. B. (2009). Analysis of thermo-visco-plastic behaviour of six high strength steels. *Materials & Design*, *30*(5), 1748-1761.

[9] Quinney, H., & Taylor, G. I. (1937). The emission of the latent energy due to previous cold working when a metal is heated. *Proceedings of the Royal Society of London. Series A, Mathematical and Physical Sciences*, 157-181.

[10] Xue, L., Mock Jr, W., & Belytschko, T. (2010). Penetration of DH-36 steel plates with and without polyurea coating. *Mechanics of materials*, *42*(11), 981-1003.

[11] R. Julien, T. Jankowiak, A. Rusinek, P. Woo, P., (2016) Taylor's Test Technique for Dynamic Characteri-zation of Materials: Application to Brass, Exp. Tech., 40, pp. 347-355.

[12] Bendarma, A., Jankowiak, T., Łodygowski, T., Rusinek, A., & Klósak, M. (2017). Experimental and numerical analysis of the aluminum alloy AW5005 behavior subjected to tension and perforation under dynamic loading. *Journal of Theoretical and Applied Mechanics*, *55*(4), 1219-1233.

[13] Recht, R., & Ipson, T. W. (1963). Ballistic perforation dynamics. *Journal of Applied Mechanics*, *30*(3), 384-390.

[14] Atkins, A. G., & Liu, J. H. (1998). Necking and radial cracking around perforations in thin sheets at normal incidence. *International journal of impact engineering*, *21*(7), 521-539.

[15] Landkof, B., & Goldsmith, W. (1985). Petalling of thin, metallic plates during penetration by cylindro-conical projectiles. *International Journal of Solids and Structures*, *21*(3), 245-266.

[16] Johnson, G. R., Cook, W. H., (1985), Fracture characteristics of three metals subjected to various strains, strain rates, temperatures and pressures. *Engineering Fracture Mechanics*, 21(1), pp. 31-48.